

Accepted Manuscript

Green flame retarding bismaleimide resin with simultaneously good processing characteristics, high toughness and outstanding thermal stability based on a multi-functional organic boron compound

Yanjing Zhu, Li Yuan, Guozheng Liang, Aijuan Gu



PII: S0141-3910(15)00135-4

DOI: [10.1016/j.polymdegradstab.2015.04.012](https://doi.org/10.1016/j.polymdegradstab.2015.04.012)

Reference: PDST 7626

To appear in: *Polymer Degradation and Stability*

Received Date: 12 February 2015

Revised Date: 29 March 2015

Accepted Date: 11 April 2015

Please cite this article as: Zhu Y, Yuan L, Liang G, Gu A, Green flame retarding bismaleimide resin with simultaneously good processing characteristics, high toughness and outstanding thermal stability based on a multi-functional organic boron compound, *Polymer Degradation and Stability* (2015), doi: 10.1016/j.polymdegradstab.2015.04.012.

This is a PDF file of an unedited manuscript that has been accepted for publication. As a service to our customers we are providing this early version of the manuscript. The manuscript will undergo copyediting, typesetting, and review of the resulting proof before it is published in its final form. Please note that during the production process errors may be discovered which could affect the content, and all legal disclaimers that apply to the journal pertain.

Green flame retarding bismaleimide resin with simultaneously good processing characteristics, high toughness and outstanding thermal stability based on a multi-functional organic boron compound

Yanjing Zhu, Li Yuan, Guozheng Liang*, Aijuan Gu*

Jiangsu Key Laboratory of Advanced Functional Polymer Design and Application

Department of Materials Science and Engineering

College of Chemistry, Chemical Engineering and Materials Science

Soochow University, Suzhou, Jiangsu 215123, China

ABSTRACT

Multi-function and green are two keywords of developing new flame retarding thermosetting resins, however, to achieve this target is still a big challenging today. Herein, a new kind of flame retarding bismaleimide resins with simultaneously good processing characteristics, high toughness and outstanding thermal stability were prepared by copolymerizing 4,4'-bismaleimidodiphenylmethane (BDM) with allyl triphenylborate (ATPB). The structure and integrated performances of BDM/ATPB resins were systematically studied and compared with the BDM/o,o'-diallylbisphenol A resin (coded as BD) that is almost known to be the best modified bismaleimide resin available. Results show that BDM/ATPB resins are solids with low softening points; they can be dissolved in acetone and have wide processing window, completely overcoming the poor processing characteristics of BDM. The properties of the BDM/ATPB system are dependent on the molar ratio of imide and allyl groups, and BDM/ATPB3 resin of which the molar ratio of imide to allyl groups (1:0.85) is the same as that of BD resin not only has significantly improved flame retardancy, reflected by obviously longer time to ignition, 1.5-3.0 times higher fire performance index, and greatly decreased heat releases, but also has about 10 °C higher initial decomposition temperature in both air and nitrogen atmospheres as well as about 1.2-1.3 times higher impact and flexural strengths, clearly demonstrating that ATPB is a multi-functional and green modifier for bismaleimide. The origin behind these attractive results of BDM/ATPB resins was intensively discussed.

Keywords: Green flame retardant; Bismaleimide resin; Organic boron-containing compound; Toughness; Mechanism

* Corresponding author. Tel: +86 512 65880967. Fax: +86 512 65880089. E-mail address: lgzheng@suda.edu.cn (Guozheng Liang); ajgu@suda.edu.cn (Aijuan Gu),

1. Introduction

As a representative of thermally resistant thermosetting resins, bismaleimide (BMI) resins have been widely used in many frontier areas owing to their outstanding thermal stability, strength and dielectric properties^[1, 2]. The most commonly used BMI is 4,4'-bismaleimidodiphenylmethane (BDM), which has high brittleness and poor processing characteristics including high melting point and narrow processing window (the gap between melting point and initial curing temperature), so during last 30 years^[3,4], a lot of researches have been focused on overcoming the two disadvantages of BDM, and great progresses have been achieved. Nowadays, multi-function and green become the trends of developing new high performance resins, of which outstanding flame retardancy has been urgently required in the fields of aerospace, electric, communication, and so on^[5-7]. Therefore, preparation of green flame retarding BMI resins is of great interesting.

Since last 10 years, lots of investigations have proved that adding non-halogen flame retardants is the main and effective method to prepare flame resistant polymers, and phosphorus flame retardants have been almost regarded as the best candidate of non-halogen flame retardants^[8,9]. However, more and more literature reported that phosphorus flame retardants produce many smoke and toxic gases (CO, NO_x, etc.); besides, phosphorus flame retardants have been not only found in indoor-air^[10], indoor-dust^[11] and drinking-water^[12], but also proved that phosphorus flame retardants may be bio-accumulated^[13-16]. Therefore developing non-halogen, non-phosphorus and environmentally-friendly flame retardants have been the most important issue.

As early as the 18th century, boric acid and borate were used as one kind of flame retardant, and have been known to have low toxicity, environmentally-friendliness, odorless and colorless^[17,18]. However, their flame retarding ability is not big even a large loading was used^[19], so they are often used as the assistant of other flame retardants for modifying polymers. Bayramlı's group^[20] discussed the influence of the sort of boron-containing compound on a intumescent system composed of ammonium polyphosphate (APP) and pentaerythritol (PER) for polypropylene (PP), they found that the best flame retarding effect was obtained with the aid of 1 wt% boron compound. Similar research was also reported by Dogan and his associates^[21].

In recent years, the preparation and modification of polymers have become noticeable. Galià's group^[22] compared the flame retardancy of soybean-based copolymers with the addition of tri-(phenylboroxine) (BAD) and that with reactive tri-(4-vinylphenylboroxine) (BST), and found that

the two kinds of boric acid esters have adverse influences on the peak of heat release rate (pHRR), specifically, the addition of BST decreased the pHRR by 20%, but the addition of BAD increased pHRR by 3 wt%, suggesting that using reactive boric acid ester is beneficial to achieve better flame retardancy.

Note that the amount of reactive groups in organic boric acid esters has been found to have effect on the thermal stability of modified polymers. The modified polymer with single functional group has much lower initial degradation temperature (T_{di}) than original polymers^[22, 23]. This problem can be solved by using boron compounds with multi-functional groups. For example, Jing's group^[24] modified bis-benzoxazine resin by introducing multi-functional hyperbranched poly(resorcinol borate), and found that the char yield of the modified resin was about 6 wt% higher than that of the original resin, meanwhile the thermal stability nearly did not changed. Cádiz's group^[25] used boron compounds with bi-functional groups to modify polystyrene, and found that with only 1.6 wt% of boron, limited oxygen index (LOI) increased from 17.2 to 20.6 %, and the T_{di} increased from 306 to 403 °C.

Above valuable studies imply that reactive boron compounds with multi-functional groups can improve the flame retardancy of polymers without sacrificing the thermal stability. However, these compounds could not be directly used to modify BMI, because their structures do not fit that of BMI. Moreover, in the case of developing new flame retardants for thermally resistant resins, the improvement of processing characteristics and toughness should be also paid attention. Therefore, designing and preparing novel flame retarding BMI resins with simultaneously improved processing characteristics, toughness and thermal stability based on green multi-functional modifier is a meaningful challenge.

In this paper, a kind of multi-functional reactive boron compound, allyl triphenylborate (ATPB), was synthesized, which was copolymerized with 4,4'-bismaleimidodiphenylmethane (BDM) to prepare a series of BDM/ATPB resins. The structure and integrated performances of BDM/ATPB resins were studied systematically. Some interesting and attractive results were obtained, the origin behind was intensively discussed.

2. Experimental section

2.1. Materials

O-Allylphenol and 2,2'-diallyl bisphenol A (DBA) with industrial grades were purchased from Laiyu Chemical Co., Ltd. (China). BDM was bought from Northwestern Chemical Engineering

Institute (China). Other reagents were commercial products with analytical grades and used without further treatment.

2.2. Synthesis of ATPB

ATPB was synthesized through the dehydration of the phenolic hydroxyl and boric acid^[26] (Figure 1). Specifically, 0.6 mol allylphenol and 0.1 mol boric acid were dissolved in toluene (50 mL) with stirring to form a mixture, which was heated to 100 °C and maintained at that temperature for 1 h, and then heated up to 130 °C with refluxing for 3 h, followed by refluxing at 160 °C for 5 h. After that, the reaction solution was cooled down to 130 °C and vacuum distilled till no liquid was evaporated from the reaction solution. Finally, a transparent, faint yellow liquid was gained, which was ATPB, its concentration of allyl groups was determined to be 0.23379 molar mass in every 100 g ATPB using the titration method^[27].

Figure 1. (single column)

2.3. Preparation of resins

According to Table 1, appropriate quantities of BDM and DBA were blended with stirring at 145 °C until a clear and brown liquid was obtained. And then the liquid was kept at 145 °C for additional 0.5 h to get a prepolymer, coded as BD. Similarly, BDM/ATPB prepolymer was prepared using above procedure except that DBA was replaced by ATPB.

Table 1.

Each prepolymer was poured into a preheated glass mold and degassed under vacuum at 145 °C for 30 min. After that, the mold was put into an oven for curing using the procedure of 150 °C/2 h + 180 °C/2 h + 200 °C/2 h + 220 °C/2 h, and followed by postcuring at 230 °C for 4 h.

2.4. Characterizations

Fourier Transform Infrared (FTIR) spectra were recorded between 400 and 4000 cm^{-1} with a resolution of 2 cm^{-1} on a Prostar LC240 Infrared Spectrometer (USA).

¹H-NMR spectra were recorded on a Bruker WM300 (Germany) with CDCl_3 as the solvent and TMS as the internal standard. ¹³C-NMR spectra were recorded on a Bruker WM300 (Germany) with CDCl_3 as the solvent and internal standard.

Differential Scanning Calorimetry (DSC) measurements were conducted on a DSC 2010 (TA Instruments, USA) ranging from room temperature to 350 °C with a heating rate 10 °C/min under a nitrogen atmosphere.

Dynamic Mechanical Analysis (DMA) scans were performed using TA DMA Q800 apparatus from TA Instruments (USA). A single cantilever clamping mode was used. DMA test were carried out from room temperature to 350 °C with a heating rate of 5 °C/min at 1 Hz. The dimensions of samples were (35 ± 0.02) mm \times (13 ± 0.02) mm \times (3 ± 0.02) mm.

Positron Annihilation Lifetime Spectroscopy (PALS) was recorded using a positron lifetime spectrometer with a fast-slow coincidence system (USA). ^{22}Na was selected as the radio active source, the spectrometer resolution was 300 ps, and cumulative counts for each spectrum were 1×10^6 . All PALS measurements were performed at 20 ± 0.5 °C under an air atmosphere. The resultant spectra were consistently modeled with a three-component fit with the computer program PATFIT-88. The dimensions of each sample were (10 ± 0.02) mm \times (10 ± 0.02) mm \times (1 ± 0.02) mm.

Thermogravimetric (TG) analyses were performed on a TA Instruments SDTQ600 (USA) under a nitrogen or air atmosphere with a flow rate of 100 mL/min and a heating rate of 10 °C/min.

LOI values were measured with a Stanton Redcraft flame meter (London, U.K.) according to ASTM D 2863/77. The dimensions of each sample were (130 ± 0.02) mm \times (6.5 ± 0.02) mm \times (3 ± 0.02) mm. Three samples were tested for each composite, the values were reproducible within 0.5%, and the average value was used as the final result.

Cone Calorimeter (CONE) tests were performed on an FTT device (UK) according to ISO 5660 with an incident flux of 35 kW/m². For each resin, three specimens were tested. Each sample was put into an aluminum boat (tray), which was then put into the specimen holder in the horizontal orientation for testing. Typical results from CONE tests were reproducible to within about $\pm 10\%$. The dimensions of each sample were (100 ± 0.02) mm \times (100 ± 0.02) mm \times (3 ± 0.02) mm.

X-ray Diffraction (XRD) reflectance patterns were obtained on a MERCURY CCD X-ray diffractometer (RIGAKU, Japan) with Cu K α radiation. The 2θ angle ranged from 5 to 60°, and the scanning rate was 2°/min.

Scanning Electron Microscope (SEM) (Hitachi S-4700, Japan) coupled with an energy disperse X-ray spectrometer (EDS) was employed to observe the morphologies of the samples. The resolution of the secondary electron image was 1.5 nm under 15 kV. All samples were dried at 100 °C for 6 h before tests.

Thermogravimetric Analysis Infrared (TG-IR) spectra were recorded using a thermogravimetric analyzer (TGA F1, Netzsch, Germany) that was interfaced to a FTIR spectrophotometer (TENSOR 27,

Bruker, Germany). Ten milligrams of a sample was put in an alumina crucible and heated from 40 to 800 °C with a heating rate of 10 °C/min under a nitrogen atmosphere, and the flowing rate was 45 mL/min.

The impact strengths were tested according to GB/T2571-1995 using a Charpy impact machine tester (XCJ-L, China), at least five samples from each formulation were broken.

The flexural strengths were measured according to GB/T2570-1995 using a electronic universal testing machine (RIGER-20, China) at a crosshead speed of 2 mm/min.

3. Results and discussion

3.1. Synthesis and characterization of ATPB

Figure 2 shows the FTIR spectra of ATPB, boric acid and allyl phenol. Compared with the spectrum of boric acid, that of ATPB does not show the characteristic absorption peak of B-OH at 1198 cm^{-1} [28], but has a new peak (1375 cm^{-1}) assigning to B-O-C [29], indicating the proceed of the dehydration between phenolic hydroxyl and boric acid as shown in Figure 1. This statement is further confirmed by the appearances of quaternary carbon signal (at 151.21 ppm) assigning to C-O-B [30] in the ^{13}C -NMR spectrum (Figure 3 left) of ATPB as well as the allyl protons (4.91-5.12 ppm) [31] in the ^1H -NMR spectrum (Figure 3 right) of ATPB. All these spectra prove the successful synthesis of ATPB.

Figure 2. (single column)

Figure 3. (2-column)

3.2. Crosslinked structures of cured BD and BDM/ATPB resins

As introduced above that BDM has poor solubility, narrow processing window and high brittleness, the modified BDM resin should overcome these defects besides the improvement of flame retardancy. Many studies have proved that allyl phenol compounds will react with BDM through the 'Diels-Alder' and 'allyl addition' reactions [32-34], and the modified BDM resins have good processing characteristics and toughness [35-37]. Therefore, a series of BDM/ATPB resins with different formulations (the molar ratio of BDM to ATPB ranged from 3:1 to 1:1) were designed to discuss the influences of the ratio on the structures and performances of resins. Meanwhile, BD resin consisting of BDM and DBA with the optimum molar ratio (1: 0.85) [38, 39], which is almost known to be the best modified BMI resin, was also prepared for comparison.

Many researches prove that BD prepolymer has good processing characteristics including good solubility in solvents that has low boiling point and low toxicity, wide processing window, this

advantage is also owned by BDM/ATPB prepolymers prepared herein. Specifically, all BDM/ATPB prepolymers have a good solubility in acetone; in addition, BDM/ATPB prepolymers are solids, their softening points are about 60 °C, the processing window is as wide as about 90 °C. All these suggest that BDM/ATPB has good processing characteristics.

It is well known that performances of a material are determined by its structure. For a thermosetting resin, its structure includes polymer chain and aggregation state structures, both of them are dependent on the curing behavior. Figure 4 depicts the DSC curves of BD and BDM/ATPB prepolymers, these curves are almost same, each of them shows an exothermic peak appearing at similar temperature range. This is expected because BD and BDM/ATPB systems have same curing mechanism, including the ‘Diels-alder’ and ‘ene addition’ reactions between allyl group and imide ring as well as the self-polymerization of BDM^[40]. Because the prepolymerization procedure is at 145 °C for 2 h, the ‘ene addition’ has been almost complete^[41], so there is sole exothermic peak in the DSC curves.

Figure 4. (single column)

To clearly evaluate the chemical structures of BDM/ATPB system, the FTIR spectra at different curing steps of BD and BDM/ATPB3 resins that have same molar ratio of imide to allyl groups were recorded. As shown in Figure 5, with the progress of curing, the absorption peaks attributing to allyl group (950 cm⁻¹) and imide ring (3200 cm⁻¹) exist in each spectrum, but their conversion degrees that compared with the vibration peak of carbonyl (A_{C=O}, at 1758 cm⁻¹) are different (Figure 6). In detail, after cured at 145 °C for 2 h, the conversion degrees of allyl and imide groups in BD reach 95.75% and 97.68%, respectively; while the conversion degree of imide group in the BDM/ATPB3 resin was only 54.79%. This difference exists along the whole curing process. For example, after postcured at 230 °C for 4 h, the conversion degrees of allyl and imide groups in BD system are as high as 98.4% and 99.7%, respectively, while those in BDM/ATPB3 are severally 92.8% and 98.3%. This difference (especially in allyl group) reflects that although BDM/ATPB3 has same molar ratio and curing mechanism as BD, the allyl groups in ATPB have lower reactivity than those in BDA, suggesting that ATPB has a steric hindrance.

Figure 5. (2-column)

Figure 6. (single column)

The aggregation state structures of thermosetting resins are often characterized by the crosslinking density ($X_{density}$) and free volume. $X_{density}$ reflects the concentration of crosslinking bonds per unit volume, the value of highly crosslinking system can be calculated based on the storage modulus (G') in rubbery state (Figure SI-1 in the Supporting Information) using a semi-empirical equation shown in Eqn (1).

$$\log_{10}G'=7+293X_{density} \quad (1)$$

Herein, G' is chosen as the modulus at the temperature that is 20 °C higher than T_g .

The calculated $X_{density}$ values are depicted in Figure 7. It can be seen that the $X_{density}$ of BDM/ATPB resin was closely related with the content of ATPB. When the loading of ATPB is small, the resins (BDM/ATPB1 and BDM/ATPB2) have higher $X_{density}$ values than BD resin, this is because BDM occupies the domain loading, and then the amount of the BDM homopolymer is large, leading to increased $X_{density}$ value. As the ATPB content enlarges, the amount of the BDM homopolymer decreases, and then the $X_{density}$ decreases. It's remarkable that BD and BDM/ATPB3 have similar $X_{density}$ values, this can be attributed to the combined roles of two opposite factors. On one hand, one ATPB molecule has three allyl groups, this concentration of crosslinking bonds per unit volume shortens the distance among crosslinking bonds, or increases the $X_{density}$. However, on the other hand, it is difficult for the three allyl groups in ATPB to react with BDM compared with the two allyl groups in DBA due to the steric hindrance, tending to lead lower $X_{density}$.

Figure 7. (single column)

Free volume is another important aspect for the aggregation state of a polymer^[42], which contains two important parameters, the average volume of free cavities (V_h) and fractional free volume (f_{app}). As shown in Figure 8, compared with BD resin, BDM/ATPB resins (especially with low concentrations of ATPB) have smaller V_h and f_{app} . For the latter, their V_h and f_{app} values increase gradually with the increase of the ATPB content; this is related to the structure formed during curing. When the content of ATPB is small, the concentration of BDM homopolymer is larger, so the polymer chains are well arranged, leading to small V_h and f_{app} . As the content of ATPB increases, the proportion of copolymerization is improved, producing a great deal of linear and branching chains, reducing the packing density, and thus increased V_h and f_{app} .

Figure 8. (single column)

3.3. Thermal stability of BDM/ATPB resins

Figure 9 shows the TG and DTG curves of cured BD and BDM/ATPB resins in a nitrogen or air atmosphere, the corresponding T_{di} , the maximum decomposition temperature (T_{max}) and the char yield (Y_c) at 800 °C are summarized in Table 2. It can be seen that except BDM/ATPB4, other BDM/ATPB resins have better degradation parameters than BD resin in either nitrogen or air atmosphere. Note that, no matter what the atmosphere is, BDM/ATPB3 has obviously higher T_{di} , T_{max} and Y_c values than BD resin, reflecting that the former has much better thermal stability than the latter. Obviously, it's beneficial to get good flame retardancy^[43], and will be confirmed in the latter part of this paper. Considering the fact that BDM/ATPB3 and BD resins have similar crosslinking density and curing mechanism, so the attractive thermal stability exhibited by BDM/ATPB3 is attributed to the thermal stable B-O bond^[44] and the material formed during the degradation. The mechanism will be verified in the latter part of this paper.

Compared with BD resin, BDM/ATPB4 has lower T_{di} , this result can be explained from the lower crosslinking density and concentration of BDM homopolymer as discussed above. However, BDM/ATPB4 still has much higher T_{max} and Y_c in the air atmosphere than BD resin, clearly demonstrating that ATPB has super ability to improve the thermal stability in an air atmosphere, this is attractive for actual applications.

Figure 9. (single column)

Table 2.

3.4. Flame retardancy of BDM/ATPB resins

To simulate the real fire of a material in a lab scale and then evaluate the flame retardancy, LOI and CONE techniques are often used^[45,46]. Figure 10 gives LOI values of BD and BDM/ATPB resins. It can be seen that the flame retardancy of BD resin belongs to the border between the combustible and flame resistant materials. While, interestingly, all BDM/ATPB resins have higher LOI values than BD resin, suggesting that BDM/ATPB resins are flame retarding materials.

With regard to BDM/ATPB resins, the LOI value decreases as the content of ATPB increases till reaches the minimum value for BDM/ATPB3, and then obviously increases, reflecting that there are opposite factors that play roles. Based on above discussion, it is known that the molar ratio of BDM to ATPB has obvious effect on the chemical structure and aggregate state structure of BDM/ATPB system.

Larger amount of BDM homopolymer and B-O bond as well as higher crosslinking density are beneficial to increase LOI. As the loading of ATPB increases, the amount of BDM homopolymer and crosslinking density decrease, so the magnitude order of LOI is BDM/ATPB1 < BDM/ATPB2 < BDM/ATPB3, but BDM/ATPB4 has the highest LOI among BDM/ATPB resins, declaring that when the loading of ATPB is enough, the B-O bond will play the decisive role in improving the flame retardancy.

Figure 10. (single column)

Table 3 summarizes the typical CONE data of BD and BDM/ATPB resins. BDM/ATPB4 has shorter time to ignition (TTI), this is in good agreement of its lower T_{di} as discussed above. Except that, other all parameters of BDM/ATPB system (especially BDM/ATPB3) are much better than those of BD resin, reflecting that ATPB is a good and reactive flame retardant. Besides TTI, fire performance index (FPI) and fire growth index (FGI) are two important parameters for evaluating the fire hazard of a material. Table 3 shows that FPI values of BDM/ATPB are 1.5-3.0 times higher than that of BD resin, meaning that ATPB has a greater ability to increase the time to flashover or the available time for escaping in a full-scale fire situation. This is also proved by FGI, that is, the FGI values of BDM/ATPB are only 66.4%-95.45% of that of BD resin, meaning that the risk of catching fire and combustion intensity decrease.

Table 3.

Figure 11 depicts the overlay curves of the heat release rate (HRR) as a function of time for all resins. BDM/ATPB resins have much lower total heat release (THR) and pHRR values than BD resin, especially, the pHRR and THR values of BDM/ATPB3 are only 53.8% and 47.0% of the data of BD, respectively, indicating that ATPB can efficiently improve the flame retardancy with only 1 wt% addition of boron element. Therefore, it is of great interesting to find the origin behind.

Figure 11. (single column)

Mass loss rate (MLR) represents the rate of mass loss in the process of degradation, and can reveal the flame retarding mechanism in condensed phase. As shown in Figure 12, except the larger mass loss of BDM/ATPB4 at initial 200 s, all BDM/ATPB resins have lower MLR values over the whole combustion process, preliminarily verifying that condensed phase plays role in the flame retarding mechanism. This statement is further confirmed by observing the digital photos of the chars after

CONE tests shown in Figure 13. In fact, BD resin obviously swell during combustion with great ablation degree, and the BD char was so thin and loose that it is easy to collapse. Oppositely, BDM/ATPB resins didn't display the swell phenomenon, and their shapes were maintained well with smooth surfaces. These phenomena will be discussed intensively in the following section.

Figure 12. (single column)

Figure 13. (single column)

Based on accident statistics, the main reason causing death in a fire is smoke and gases^[47], so the properties on the smoke releasing and the production of CO (toxic gas) are significant aspects of flame retardancy. The smoke releasing ability can be reflected by the smoke release rate (SPR)-time plot and specific extinction area (SEA). As shown in Figure 14 and Table 3, BDM/ATPB resins have much smaller SPR, total smoke release (TSR), total smoke production (TSP) and SEA values as well as CO production than BD resin, demonstrating that ATPB is not only an efficient flame retardant, but also a fine and green smoke suppressant.

Figure 14. (single column)

3.5. Flame retarding mechanism

Lots of researches show that flame retardants play roles through the reactions in condensed phase and/or gaseous phase, so the flame retarding effect of ATPB was studied through the two phases. The investigation on the condensed phase consists of the mass loss and char structure, while that on the gaseous phase is carried out by using the TG-IR technique. Because BD and BDM/ATPB3 resins have same ratio of imide and allyl groups, so choosing them as the models for studying can exclude the influence of the ratio on the properties, and thus is beneficial to get the flame retarding mechanism.

Figure 15 presents the digital photos of BD and BDM/ATPB3 resins after being maintained at different temperature for 15 min in a muffle furnace. BD resin cannot retain its shape after maintained at the temperature higher than 350 °C, and its volume expands fast and greatly when the temperature reaches 400 °C, moreover, the mass loses sharply with the increase of the temperature. When the temperature is up to 500 °C, the char of BD resin becomes fluffy with many holes, reflecting that the compact char could not be formed during the heating process, and thus the degradation could not be prevented. With further increased temperature, BD resin burns up. For the sample after maintained at 600 °C for 15 min, the residual mass is only 1.0 wt%, and no peak attributing to organic groups can be

observed in FTIR spectrum (Figure 16). However, BDM/ATPB3 resin can still keep its shape at 350 °C, and when the temperature is 400 °C, the sample expands, but the rectangle figure is still maintained with compact state. This condition is held till the temperature is 550 °C. After stayed at 650 °C for 15 min, the residual mass of BDM/ATPB3 resin is still as high as 10.59 wt%, in which there are organic compositions reflected by the appearance of the characteristic absorptions of organic bonds in its FTIR spectrum (Figure 16), including the imide ring (3440 cm^{-1}), the vibration stretching of C-H (2920 cm^{-1}) and the vibration stretching of CH=CH (1600 cm^{-1}), so the organic components in the BDM/ATPB system are protected well.

Figure 15. (single column)

Figure 16. (2-column)

Note that in the FTIR spectrum of the BDM/ATPB3 char after maintained at 650 °C, new peaks appear at 1200 and 782 cm^{-1} , which are assigning to the stretching vibrations of B-O in boron oxide [48,49]. This is further confirmed by the new sharp peak belonging to B_2O_3 at $2\theta=27.8^\circ$ [50,51] in the XRD pattern of BDM/ATPB3 char (Figure 17). As boron oxide is a new material that is produced during the degradation, so which is believed to make contribution to the outstanding flame retardancy of the BDM/ATPB system.

Figure 17. (2-column)

Figure 18 shows the SEM micrographs of surfaces of BD and BDM/ATPB3 chars. Compared with the images of BD char (Figures 18a, 18b), that of BDM/ATPB3 char is more condensed and looks like a net framework (Figures 18c, 18d), this is in good agreement with the compact and smooth surfaces (Figures 13 and 15).

According to all results and discussion above, it's believed that the condensed phase is one important flame retarding mechanism.

Figure 18. (single column)

TG-IR technique that directly gives identification of the volatilized products can significantly contribute to an understanding of thermal degradation mechanism [52]. Figure 19 shows the three-dimensional FTIR spectra of gaseous volatiles evolved during the whole combustion processes of BD and BDM/ATPB resins. Because samples with same size, shape and weight were used for tests, the

absorption intensity of peaks is reasonable to evaluate the relative amount of the pyrolysis products^[53].

It can be seen that BDM/ATPB resins released fewer volatilized products than BD resin.

Figure 19. (2-column)

Figure 20 gives the FTIR spectra of each sample at typical temperatures. For BD resin, a slight absorption peak assigning to CO₂ (674, 2362, 2313 cm⁻¹) is observed in the spectrum at 380 °C. At T_{di} (406 °C), the CO₂ peak is enhanced and the peak for O-H bond (3650 cm⁻¹, relating to H₂O generation) appears. When the temperature reaches T_{max} (434 °C), besides the strengthened peak of O-H bond, more peaks emerge, including aromatic compounds (3037 cm⁻¹), aliphatic components (2933 cm⁻¹), carbonyl compounds (1758 cm⁻¹), esters (1174 cm⁻¹) and nitrogen oxides (1509 cm⁻¹), indicating that the polymer chains have been fractured, and some esters coupled with the generation of CO₂ and NO_x have been formed. Note that the peaks for CO₂ and NO_x are still found even the temperature reaches 800 °C, demonstrating the continuous degradation of the resin.

Comparatively, BDM/ATPB resins show obviously different degradation behavior from BD resin. Take BDM/ATPB3 as an example, it has good thermal stability when the temperature is 380 °C. When the temperature reaches T_{di} (411 °C), the peaks for CO₂ (670, 2362, 2313 cm⁻¹), H₂O (3500-3900 cm⁻¹), and aromatic rings (1300-1650 cm⁻¹) emerge, reflecting the degradation of aromatic ring. When the temperature comes to T_{max} (431 °C), the amount of released CO₂ achieves the maximum, meanwhile new peaks assigning to phenol-containing compounds (3037 cm⁻¹), aliphatic components (2933 cm⁻¹) and C-C(=O)-O (1174 cm⁻¹) appear. As the temperature reaches 550 °C, the intensities of peaks decrease obviously. At 800 °C, almost no peaks are observed in the FTIR spectrum, this is opposite from the situation of BD resin at 800 °C. The TG curves from TG-IR tests (Figure 21) show that the Y_c of BDM/ATPB3 at 800 °C is above 50 wt%, about 2.2 times larger than that of BD, further proving that the appearance of ATPB can promote the formation of a stable protective char, and thus protecting the resin from degradation.

Figure 20. (2-column)

Figure 21. (2-column)

Above results demonstrate that the flame retarding effect of ATPB mainly focuses on the condense-phase, including improving the thermal stability, increasing the ability of char formation, and ameliorating the compactness of the char; besides, B₂O₃ are produced during degradation. All these are

beneficial to get good flame retardancy.

3.6. Mechanical properties of BDM/ATPB resins

As stated in the introduction part, toughening has been one of most important targets of the research and development of thermosetting resins. Therefore, it is of great interesting to investigate the toughness of BDM/ATPB resins. Impact strength reflects the ability to absorb the energy of a rapidly applied load, and the ability to withstand this sudden impact ^[54], so which is usually used to characterize the toughness of a material. Figure 22 presents the impact strengths of cured BD and BDM/ATPB resins. All BDM/ATPB resins have higher impact strengths than BD resin, and the impact strength increases as the content of ATPB increases. Especially, BDM/ATPB3 has about 1.3 times larger impact strength than BD resin. This is originated from the difference in the structure of the crosslinked networks between BD and BDM/ATPB resins. In the case of BD and BDM/ATPB3 resins, they have similar crosslinking density, V_h and f_{app} , so the chemical difference induced by the special ATPB is responsible for the performances. Specifically, ATPB has flexible B-O chain, and its steric hindrance makes low conversion degrees of allyl and imide groups. These will lead to the increased impact strength. As these influences are enhanced as the loading of ATPB increases, so the impact strength increases as the loading of ATPB increases. Because of the same reasons, BDM/ATPB resins have lower flexural moduli than BD resin (Figure 23).

Figure 22. (single column)

Flexural strength is often regarded as the index of mechanical properties because the flexural loading contains multi-type loadings such as tensile, shearing and/or compressing loading ^[55]. Generally, the flexural strength is dependent on both toughness and stiffness. As shown in Figure 23, all BDM/ATPB resins have higher flexural strengths than BD resin; and with the increase of ATPB content, the flexural strength rises and reaches the maximum (137 MP) for BDM/ATPB3, about 1.3 times of that of BD resin.

Figure 23. (single column)

4. Conclusions

ATPB is a green and multi-functional modifier for BDM, the presence of which not only completely overcomes the poor processing characteristics of BDM, but also endows BDM with outstanding flame retardancy, high impact and flexural strengths as well as improved thermal stability.

These attractive integrated performances of BDM/ATPB system are contributed to its structure. BDM/ATPB and BD have same curing mechanism; however, their crosslinked networks have different chemical and aggregate structures, including the crosslinking density, free volume, the proportion of homopolymer of BDM and copolymer of BDM and ATPB. The flame retarding effect of ATPB mainly plays role in the condense-phase, including improving the thermal stability, increasing the ability of char formation and the compactness of the char as well as producing B_2O_3 . This investigation provides a new method to prepare green flame retardants with multi-functions and corresponding high performance resins.

Acknowledgments

The authors thank the National Natural Science Foundation of China (21274104) and the Priority Academic Program Development of Jiangsu Higher Education Institutions (PAPD) for financially supporting this project.

Appendix A. Supplementary data

The following is the supplementary data related to this article:

Figure SI-1.

References

- [1] Lin QL, Dong SH, Qu LJ, Fang CQ, Luo K. Preparation and properties of carbon foam by direct pyrolysis of allyl novolak-modified bismaleimide resin. *J Anal Appl Pyrol* 2014; 106:164-170.
- [2] Yu Q, Chen P, Gao Y, Ma KM, Lu C, Xiong XH. Effects of electron irradiation in space environment on thermal and mechanical properties of carbon fiber/bismaleimide composite. *Nucl Instrum Meth B* 2014; 336:158-162.
- [3] Zhuo DX, Gu AJ, Liang GZ, Hu JT, Yuan L, Chen XX. Flame retardancy materials based on a novel fully end-capped hyperbranched polysiloxane and bismaleimide/diallylbisphenol A resin with simultaneously improved integrated performance. *J Mater Chem* 2011; 21:6584-6594.
- [4] Zhang Y, Lv JJ, Liu YJ. Preparation and characterization of a novel fluoride-containing bismaleimide with good processability. *Polym Degrad Stab* 2012; 97:626-631.
- [5] Xu JZ, He ZM, Wu WH, Ma HY, Xie JX, Qu HQ, et al. Study of thermal properties of flame retardant epoxy resin treated with hexakis[*p*-(hydroxymethyl)phenoxy]cyclotriphosphazene. *J Therm Anal Calorim* 2013; 114:1341-1350.
- [6] Chen XX, Ye JH, Yuan L, Liang GZ, Gu AJ. Multi-functional ladderlike polysiloxane: synthesis,

characterization and its high performance flame retarding bismaleimide resins with simultaneously improved thermal resistance, dimensional stability and dielectric. *J Mater Chem A* 2014; 2:7491-7501.

[7] Zhang T, Yan HQ, Shen L, Fang ZP, Zhang XM, Wang JJ, et al. Chitosan/phytic acid polyelectrolyte complex: a green and renewable intumescent flame retardant system for ethylene-vinyl acetate copolymer. *Ind Eng Chem Res* 2014; 53: 19199-19207.

[8] Benin Vladimir, Gardelle B, Morgan AB. Heat release of polyurethanes containing potential flame retardants based on boron and phosphorus chemistries. *Polym Degrad Stab* 2014; 106:108-121.

[9] Dorez G, Taguet A, Ferry L, Cuesta JL. Phosphorous compounds as flame retardants for polybutylene succinate/flax biocomposite: Additive versus reactive route. *Polym Degrad Stab* 2014; 102:152-159.

[10] Hartmann PC, Bürgi D, Giger W. Organophosphate flame retardants and plasticizers in indoor air. *Chemosphere* 2004; 57:781-787.

[11] Van den Eede N, Dirtu AC, Neels H, Covaci A. Analytical developments and preliminary assessment of human exposure to organophosphate flame retardants from indoor dust. *Environ Int* 2011;37: 454-461.

[12] Stackelberg PE, Gibs J, Furlong ET, Meyer MT, Zaugg SD, Lippincott RL. Efficiency of conventional drinking-water-treatment processes in removal of pharmaceuticals and other organic compounds. *Sci Total Environ* 2007; 377:255-272.

[13] Van der Veen I, De Boer J. Phosphorus flame retardants: properties, production, environmental occurrence, toxicity and analysis. *Chemosphere* 2012; 88:1119-1153.

[14] Regnery J, Püttmann W. Organophosphorus flame retardants and plasticizers in rain and snow from middle Germany. *Clean-Soil Air Water* 2009; 37:334-342.

[15] Andresen JA, Grundmann A, Bester K. Organophosphorus flame retardants and plasticisers in surface waters. *Sci Total Environ* 2004; 332:155-156.

[16] Ni Y, Kumagai K, Yanagisawa Y. Measuring emissions of organophosphate flame retardants using a passive flux sampler. *Atmos Environ* 2007; 41:3235-3240.

[17] Baysal E, Yalinkilic MK, Altinok M, Sonmez A, Peker H, Colak M. Some physical, biological, mechanical, and fire properties of wood polymer composite (WPC) pretreated with boric acid and borax mixture. *Constr Build Mater* 2007; 21:1879-1885.

[18] Kurt R, Mengeloğlu F. Utilization of boron compounds as synergists with ammonium

- polyphosphate for flame retardant wood-polymer composites. *Turk J Agric For* 2011; 35:155-163.
- [19] Martín C, Ronda JC, Cádiz V. Development of novel flame-retardant thermosets based on boron-modified phenol-formaldehyde resins. *J Polym Sci Pol Chem* 2006; 44:3503-3512.
- [20] Doğan M, Yılmaz A, Bayramlı E. Synergistic effect of boron containing substances on flame retardancy and thermal stability of intumescent polypropylene composites. *Polym Degrad Stab* 2010; 95:2584-2588.
- [21] Dogan M, Unlu SM. Flame retardant effect of boron compounds on red phosphorus containing epoxy resins. *Polym Degrad Stab* 2014; 99:12-17.
- [22] Sacristán M, Hull TR, Stec AA, Ronda JC, Galià M, Cádiz V. Cone calorimetry studies of fire retardant soybean-oil-based copolymers containing silicon or boron: Comparison of additive and reactive approaches. *Polym Degrad Stab* 2010; 95:1269-1274.
- [23] Martín C, Ronda JC, Cádiz V. Boron-containing novolac resins as flame retardant materials. *Polym Degrad Stab* 2006; 91:747-754.
- [24] Si JJ, Xu PJ, He W, Wang SJ, Jing XL. Bis-benzoxazine resins with high char yield and toughness modified by hyperbranched poly(resorcinol borate). *Compos Part A-Appl S* 2012; 43:2249-2255.
- [25] Martín C, Hunt BJ, Ebdon JR, Ronda JC, Cádiz V. Synthesis, crosslinking and flame retardance of polymers of boron-containing difunctional styrenic monomers. *React Funct Polym* 2006; 66:1047-1054.
- [26] Wang DC, Chang GW, Chen Y. Preparation and thermal stability of boron-containing phenolic resin/clay nanocomposites. *Polym Degrad Stab* 2008; 93:125-133.
- [27] Espiard P, Mark JE, Guyot A. A novel technique for preparing organophilic silica by water-in-oil microemulsions. *Polym Bull* 1990; 24:173-179.
- [28] Yanase I, Ogawara R, Kobayashi H. Synthesis of boron carbide powder from polyvinyl borate precursor. *Mater Lett* 2009; 63:91-93.
- [29] Majoni S, Su SP, Hossenlopp JM. The effect of boron-containing layered hydroxy salt (LHS) on the thermal stability and degradation kinetics of poly (methyl methacrylate). *Polym Degrad Stab* 2010; 95:1593-1604.
- [30] Martín C, Ronda JC, Cádiz V. Boron-containing novolac resins as flame retardant materials. *Polym Degrad and Stab* 2006; 91:747-754.
- [31] Liu YF, Liao CY, Hao ZZ, Luo XX, Jing SS, Run MT. The polymerization behavior and thermal

properties of benzoxazine based on *o*-allylphenol and 4,4'-diaminodiphenyl methane. *Reac Funct Polym* 2014; 75:9-15.

[32] Frias CF, Fonseca AC, Coelho JFJ, Serra AC. Straightforward functionalization of acrylated soybean oil by Michael-addition and Diels-Alder reactions. *Ind Crop Prod* 2015; 64:33-38.

[33] Shibata M, Tetramoto N, Imada A, Neda M, Sugimoto S. Bio-based thermosetting bismaleimide resins using eugenol, bieugenol and eugenol novolac. *React Func Polym* 2013; 73:1086-1095.

[34] Gaina C, Ursache O, Gaina V, Musteata VE. High performance thermosets based on multifunctional intermediates containing allyl, maleimide and benzoxazine groups. *J Polym Res* 2013; 20:263-273.

[35] Liu HY, Lin QL, Li YF, Luo B, Fang CQ. Preparation of near net-shape carbon foams from allyl COPNA-modified bismaleimide resin. *J Anal Appl Pyro* 2014; 110:476-480.

[36] Ursache O, Gaina C, Gaina V, Musteata VE. High performance bismaleimide resins modified by novel allyl compounds based on polytriazoles. *J Polym Res* 2012; 19:9968-9976.

[37] Tang HY, Fan XH, Shen ZH, Zhou QF. One-pot synthesis of hyperbranched poly(aryl ether ketone)s for the modification of bismaleimide resins. *Polym Eng Sci* 2014; 54:1675-1685.

[38] Jin JY, Cui J, Tang XL, Ding YF, Li SJ, Wang JC, et al. On polyetherimide modified bismaleimide resins, 1. effect of the chemical backbone of polyetherimide. *Macromol Chem Phys* 1999; 200:1956-1960.

[39] Liu XY, Yu YF, Li SJ. Viscoelastic phase separation in polyethersulfone modified bismaleimide resin. *Eur Polym J* 2006; 42:835-842.

[40] Liang GZ, Hu XL. Aluminum-borate-whiskers-reinforced bismaleimide composites. 1: preparation and properties. *Polym Int* 2004; 53:670-674.

[41] Tang HY, Li WW, Fan XH, Chen XF, Shen ZH, Zhou QF. Synthesis, preparation and properties of novel high-performance allyl-maleimide resins. *Polymer* 2009; 50:1414-1422.

[42] Chang KS, Huang YH, Lee KR, Tung KL. Free volume and polymeric structure analyses of aromatic polyamide membranes: A molecular simulation and experimental study. *J Membrane Sci* 2010; 354:93-100.

[43] Realinho V, Haurie L, Antunes M, Velasco JI. Thermal stability and fire behaviour of flame retardant high density rigid foams based on hydromagnesite-filled polypropylene composites. *Compos Part B-Eng* 2014; 58:553-558.

- [44] Gao JG, Liu YF, Yang LT. Thermal stability of boron-containing phenol formaldehyde resin. *Polym Degrad Stab* 1999; 63:19-22.
- [45] Li Z, Wei P, Yang Y, Yan YY, Shi D. Synthesis of a hyperbranched poly(phosphamide ester) oligomer and its high-effective flame retardancy and accelerated nucleation effect in polylactide composites. *Polym Degrad Stab* 2014; 110:104-112.
- [46] Zhou Y, Feng J, Peng H, Qu HQ, Hao JW. Catalytic pyrolysis and flame retardancy of epoxy resins with solid acid boron phosphate. *Polym Degrad Stab* 2014; 110:395-404.
- [47] Chen XL, Huo LL, Jiao CM, Li SX. TG-FTIR characterization of volatile compounds from flame retardant polyurethane foams materials. *J Anal Appl Pyrol* 2013; 100:186-191.
- [48] Ardelean I, Cora S, Rusu D. EPR and FT-IR spectroscopic studies of $\text{Bi}_2\text{O}_3\text{-B}_2\text{O}_3\text{-CuO}$ glasses. *Physica B* 2008; 403:3682-3685.
- [49] Doweidar H, El-Damrawi G, Mansour E, Fetouh RE. Structure role of MgO and PbO in $\text{MgO-PbO-B}_2\text{O}_3$ glasses as revealed by FTIR: a new approach. *J Non-cryst Solid* 2012; 358:941-946.
- [50] Zhu LY, Wang XQ, Zhang GH, Ren Q, Xu D. Structure characterization and photocatalytic activity of $\text{B}_2\text{O}_3/\text{ZrO}_2\text{-TiO}_2$ mesoporous fibers. *Appl Catal B- Environ* 2011; 103:428-435.
- [51] Al-Rashdi B, Tizaoui C, Hilal N. Copper removal from aqueous solutions using nano-scale diboron trioxide/titanium dioxide ($\text{B}_2\text{O}_3/\text{TiO}_2$) adsorbent. *Chem Eng J* 2012; 183:294-302.
- [52] Chen XL, Jiao CM. Thermal degradation characteristics of a novel flame retardant coating using TG-IR technique. *Polym Degrad Stab* 2008; 93:2222-2225.
- [53] Jin WQ, Yuan L, Liang GZ, Gu AJ. Multifunctional cyclotriphosphazene/hexagonal boron nitride hybrids and their flame retarding bismaleimide resins with high thermal conductivity and thermal stability. *ACS Appl Mater Inter* 2014; 6:14931-14944.
- [54] Ye JH, Liang GZ, Gu AJ, Zhang ZY, Han JP, Yuan L. Novel phosphorus-containing hyperbranched polysiloxane and its high performance flame retardant cyanate ester resins. *Polym Degrad Stab* 2013; 98:597-608.
- [55] Xavier SF, Misra A. Influence of glass fiber content on the morphology and mechanical properties in injection molded polypropylene composites. *Polym Compos* 1985; 6:93-99.

Figure Captions

Figure 1. Synthesis of ATPB

Figure 2. FTIR spectra of ATPB, allylphenol and boric acid

Figure 3. The ^{13}C -NMR (left) and ^1H -NMR (right) spectra of ATPB

Figure 4. DSC curves of BD and BDM/ATPB prepolymers

Figure 5. FTIR spectra of BD and BDM/ATPB3 resins cured at different stages: (1) 145 °C/2h, (2) 145 °C/2h+150 °C/2h, (3) 145 °C/2h+150 °C/2h+180 °C/2h, (4) 145 °C/2h+150 °C/2h+180 °C/2h+200 °C/2h, (5) 145 °C/2h+150 °C/2h+180 °C/2h+200 °C/2h+220 °C/2h, (6) 145 °C/2h+150 °C/2h+180 °C/2h+200 °C/2h+220 °C/2h+230 °C/4h

Figure 6. Conversion degrees of allyl and imide ring groups in BD and BDM/ATPB3 resins cured at different stages

Figure 7. Crosslinking densities of cured BD and various BDM/ATPB resins

Figure 8. V_h and f_{app} values of BD and BDM/ATPB resins

Figure 9. TG (a, c) and DTG (b, d) curves of cured BD and BDM/ATPB resins under a nitrogen (a, b) or an air (c, d) atmosphere

Figure 10. LOI values of BD and BDM/ATPB resins

Figure 11. Overlay plots of dependence of HRR on time for BD and BDM/ATPB resins

Figure 12. Overlay plots of dependence of normalized mass loss on time for BD resin and BDM/ATPB resins

Figure 13. Digital photos of chars of BD and BDM/ATPB resins after CONE tests

Figure 14. Overlay plots of dependence of SPR on time for BD and BDM/ATPB resins

Figure 15. Digital photos of BD and BDM/ATPB3 resins after maintained at different temperature for 15 min in a muffle furnace

Figure 16. FTIR spectra of the chars of BD and BDM/ATPB resins after maintained at different temperatures for 15 min in a muffle furnace

Figure 17. XRD spectra of original and residual samples (a: BD; b: BDM/ATPB3)

Figure 18. SEM images of the chars of BD resin (a: 10K magnification; b: 1K magnification) and BDM/ATPB3 resin (c: 10K magnification; d: 1K magnification)

Figure 19. Three-dimensional FTIR spectra of the gaseous volatiles evolved during the combustion

process of BD and BDM/ATPB resins in a N₂ atmosphere

Figure 20. FTIR spectra of volatilized products at typical temperatures for BD and BDM/ATPB resins

Figure 21. TG curves for BD and BDM/ATPB3 resins from TG-IR tests

Figure 22. Dependence of the content of ATPB on the impact strength of cured BD and BDM/ATPB

Figure 23. Flexural strengths and moduli of BD and BDM/ATPB resins

ACCEPTED MANUSCRIPT

Table 1. Formulations of BD and BDM/ATPB resins

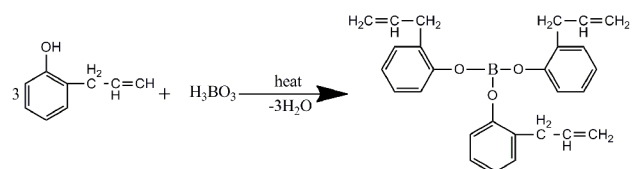
Resin	Mass ratio			Molar ratio of imide to allyl groups		
	BDM	DBA	ATPB	BDM	DBA	ATPB
BD	58	42	0	1	0.85	0
BDM/ ATPB1	58	0	25	1	0	0.55
BDM/ ATPB2	58	0	32	1	0	0.70
BDM/ ATPB3	58	0	39	1	0	0.85
BDM/ ATPB4	58	0	46	1	0	1.00

Table 2. Typical parameters from TG analyses of cured BD and BDM/ATPB resins

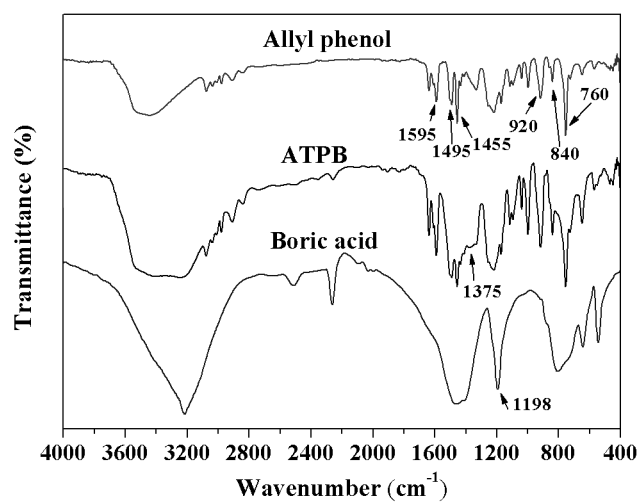
Resin	Atmosphere	T_{di} (°C)	T_{max} (°C)		Y_c at 800 °C (wt%)
			T_{max1} (°C)	T_{max2} (°C)	
BD		406.4	434.3	--	26.1
BDM/ATPB1		428.1	440.7	--	55.9
BDM/ATPB2	Nitrogen	425.3	435.6	--	57.9
BDM/ATPB3		416.4	433.0	--	55.1
BDM/ATPB4		380.2	433.0	--	52.6
BD		401.8	433.7	580.4	0.00
BDM/ATPB1		431.4	440.0	646.3	25.56
BDM/ATPB2	Air	426.5	443.4	641.9	19.64
BDM/ATPB3		414.3	434.0	635.5	16.56
BDM/ATPB4		370.4	436.3	634.2	17.18

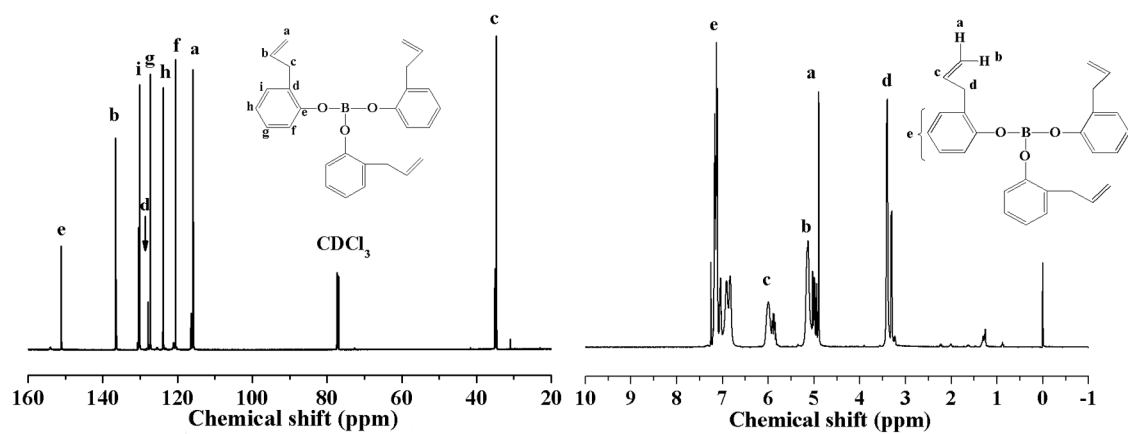
Table 3. Typical Parameters for BD and BD/ATPB resins from CONE Tests

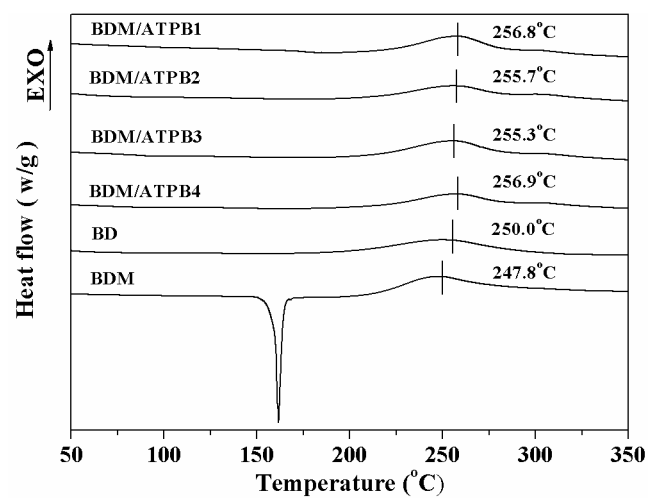
Property	BD	BDM/ATPB1	BDM/ATPB2	BDM/ATPB3	BDM/ATPB4
TTI (s)	95	164	162	111	63
FPI (s•m ² /kW)	0.36	1.09	0.82	0.79	0.55
FGI (kW/(m ² •K))	1.10	0.73	1.05	0.97	0.87
MLR (g/s)	0.055	0.030	0.029	0.027	0.035
SEA (m/kg)	725.5	237.4	316.0	393.0	418.3
TSR (m ² /m ²)	2510.5	340.6	528.2	584.2	952.9
TSP (m ²)	22.19	3.01	4.67	5.16	8.42
CO (kg/kg)	0.070	0.039	0.050	0.035	0.038



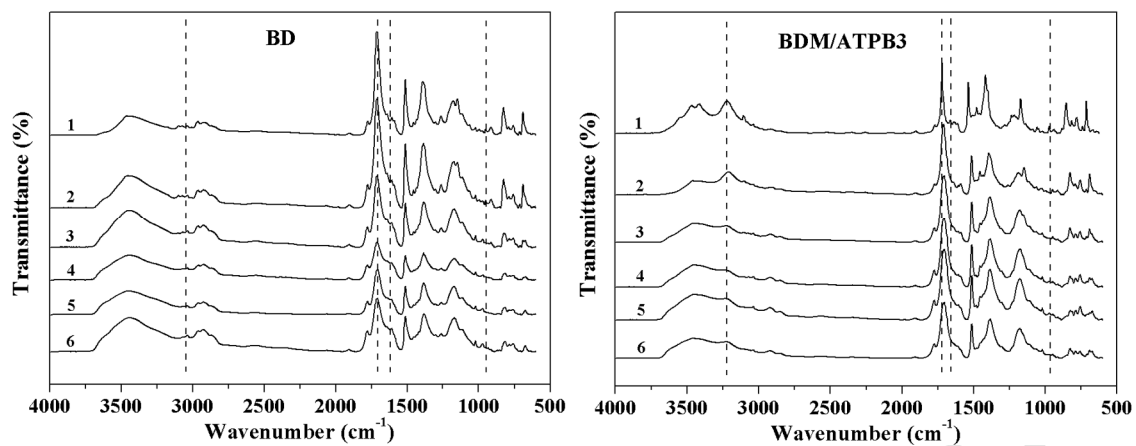
ACCEPTED MANUSCRIPT

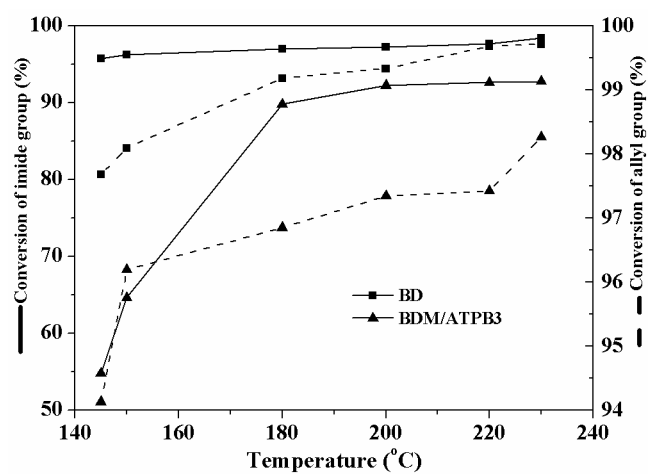


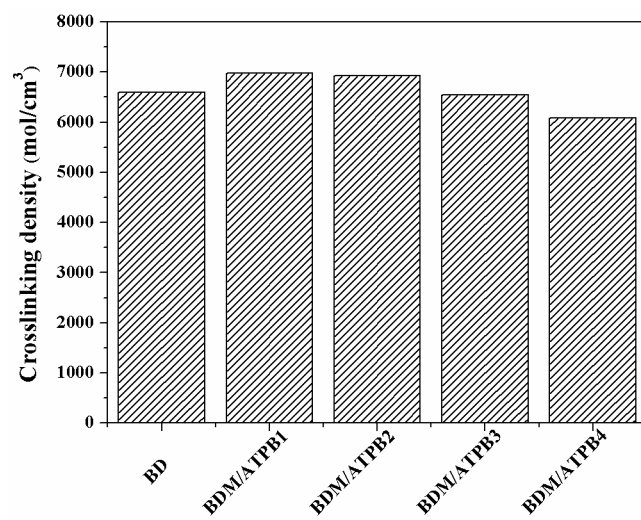


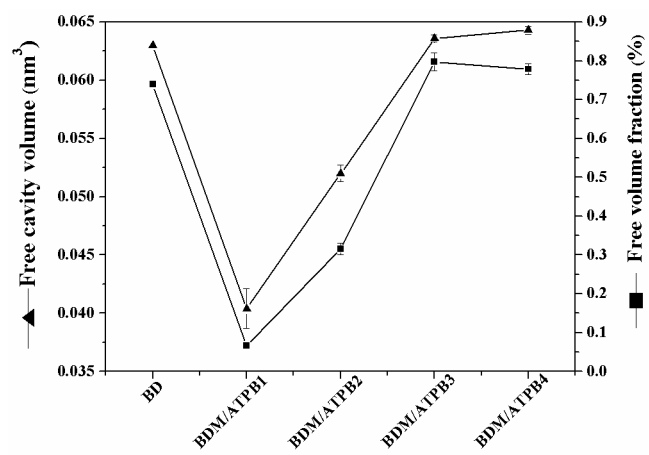


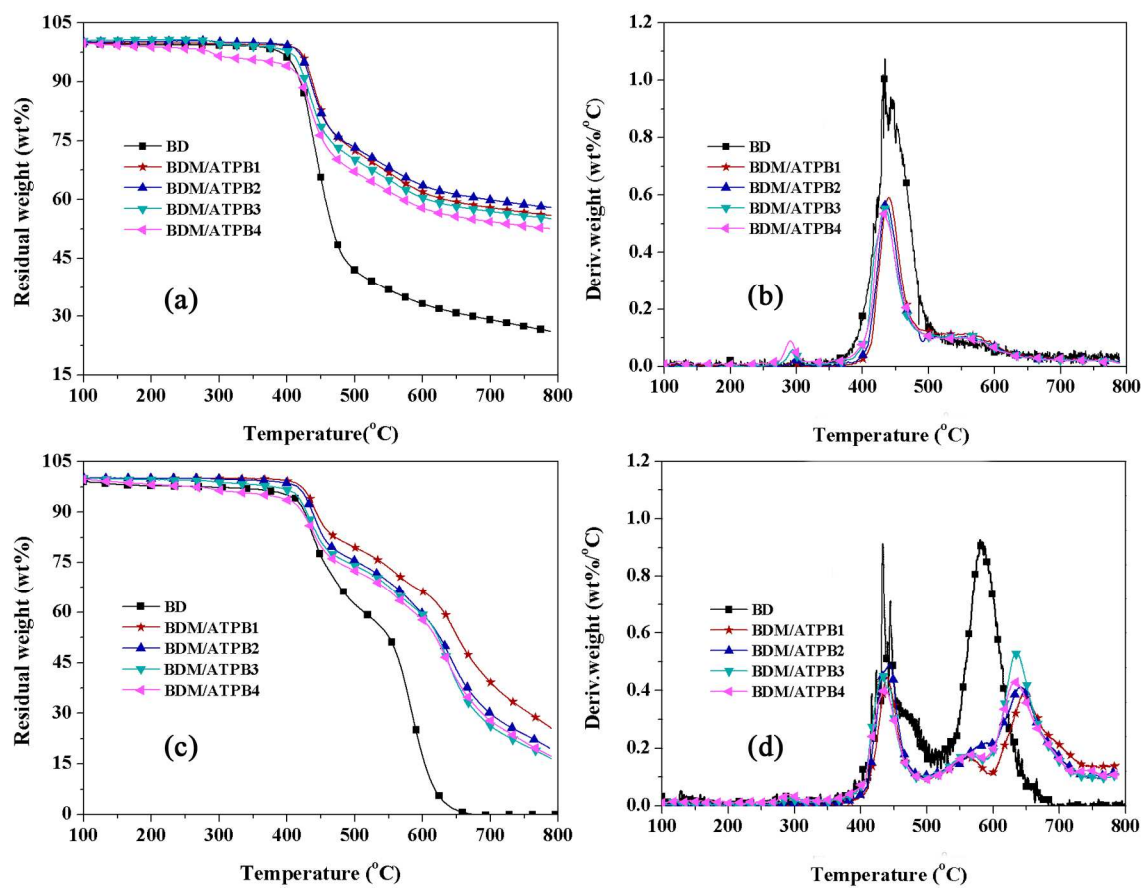
ACCEPTED MANUSCRIPT

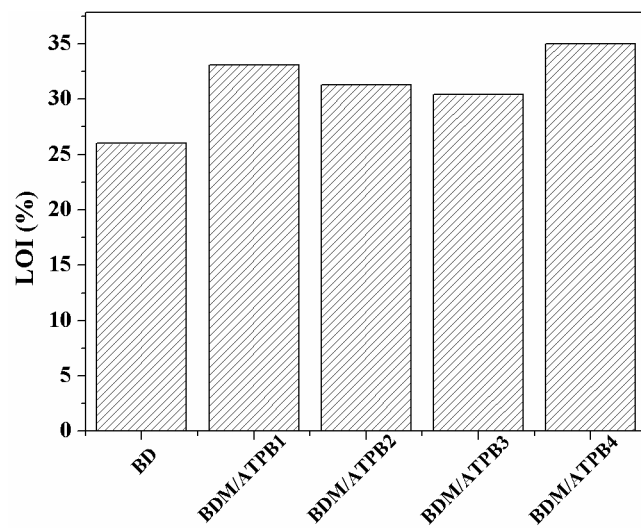


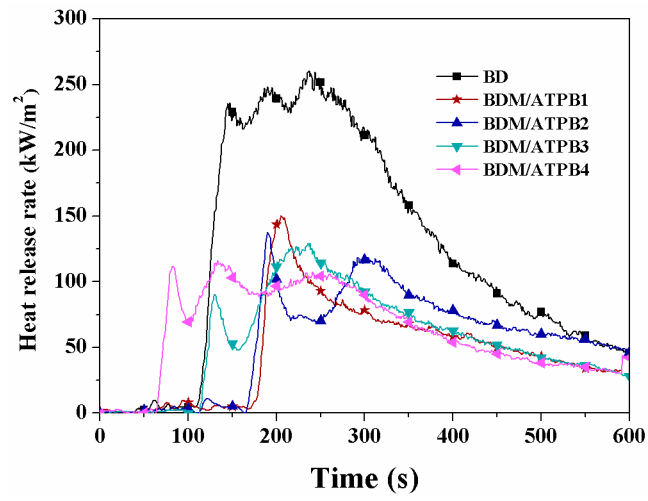


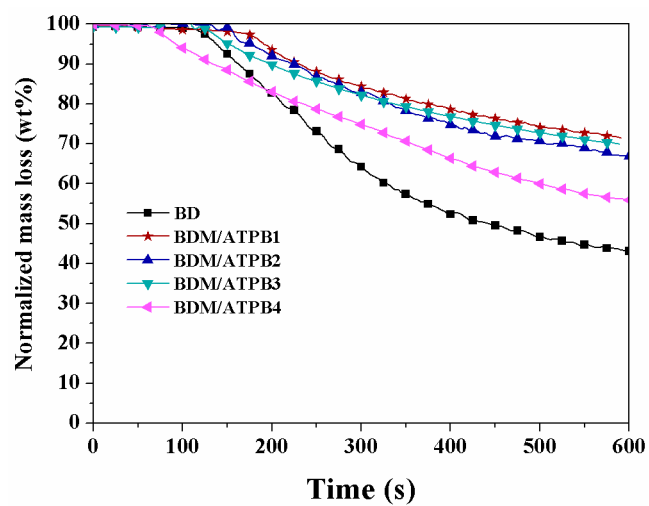


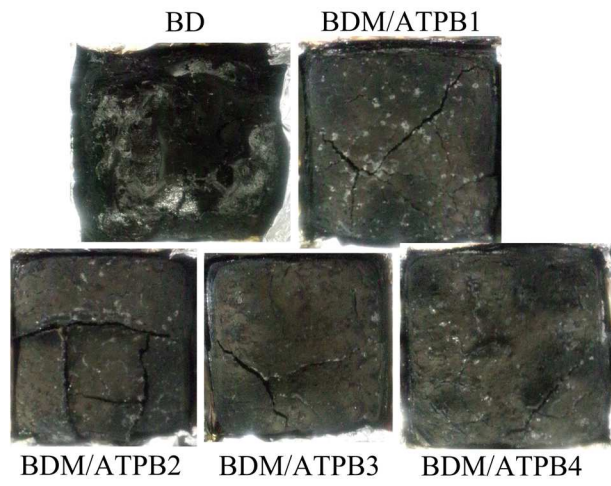


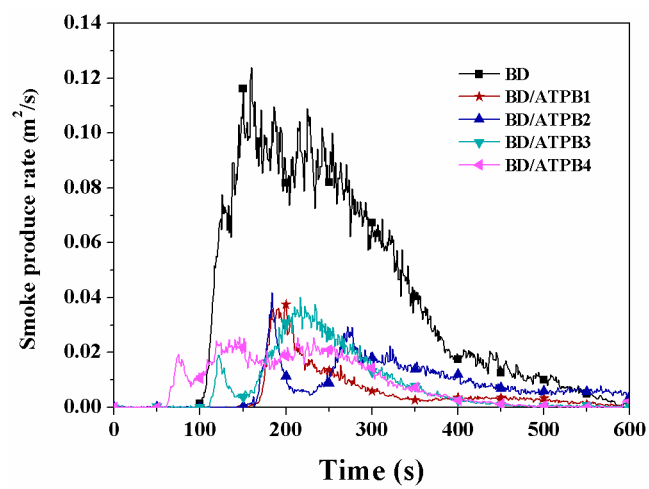


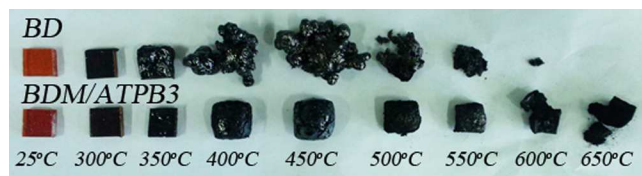




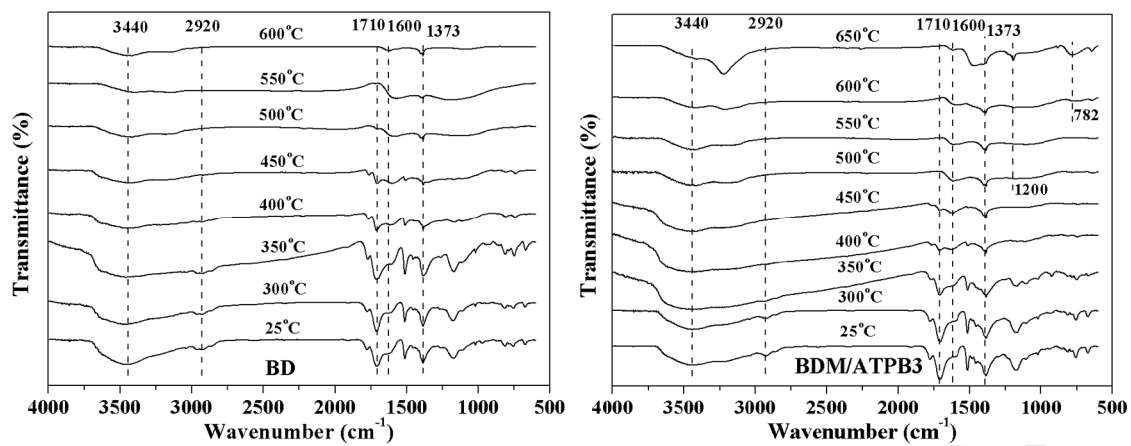


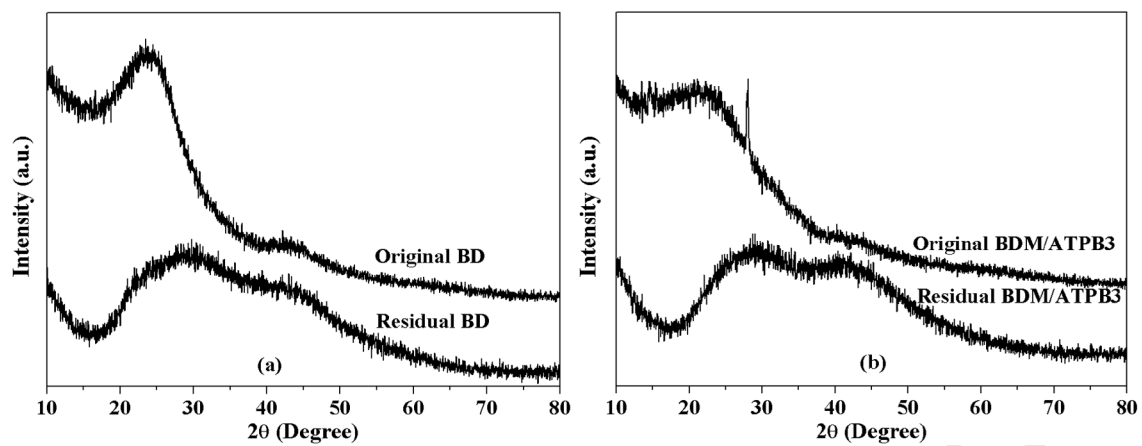


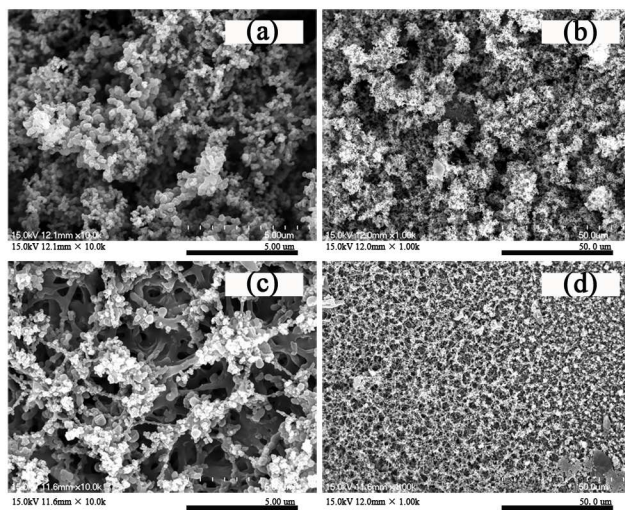


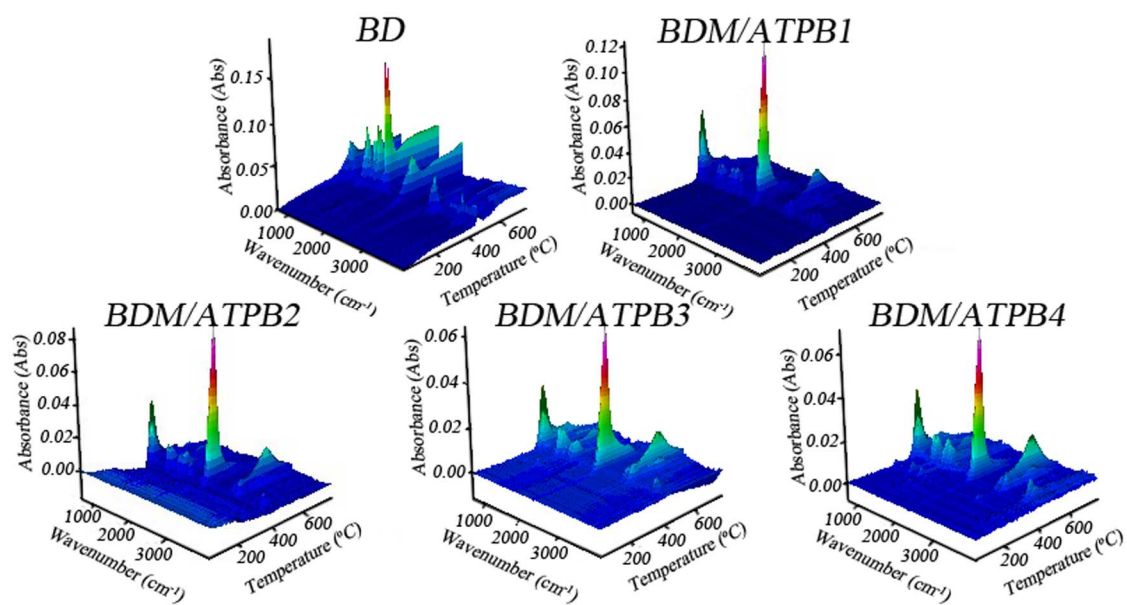


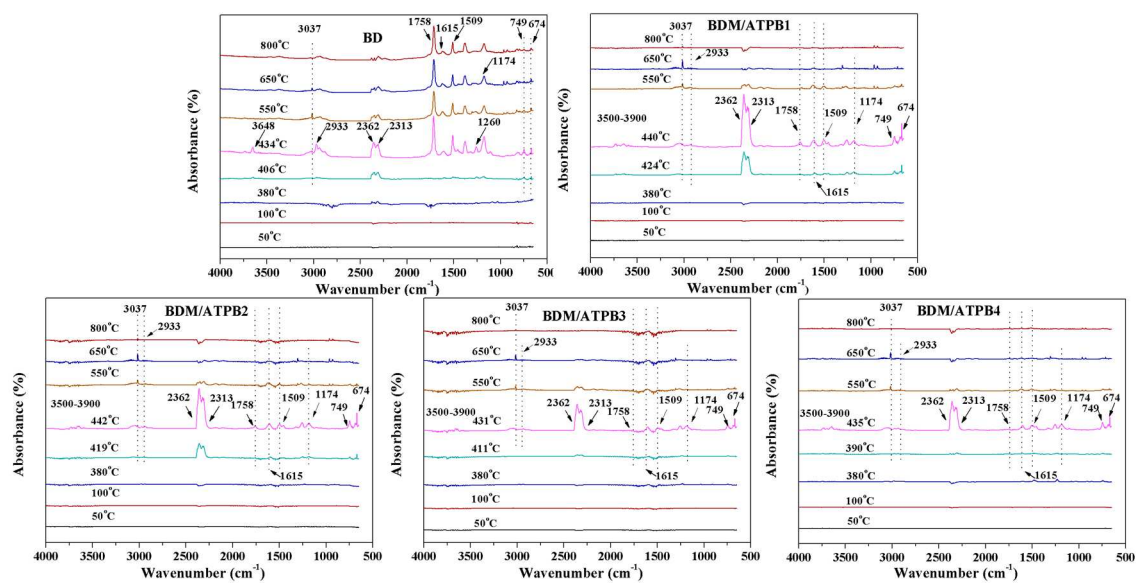
ACCEPTED MANUSCRIPT

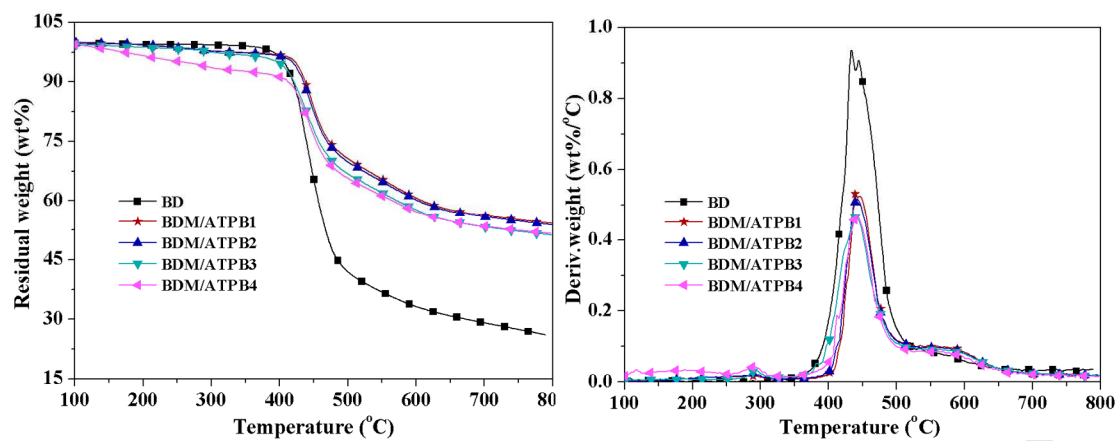


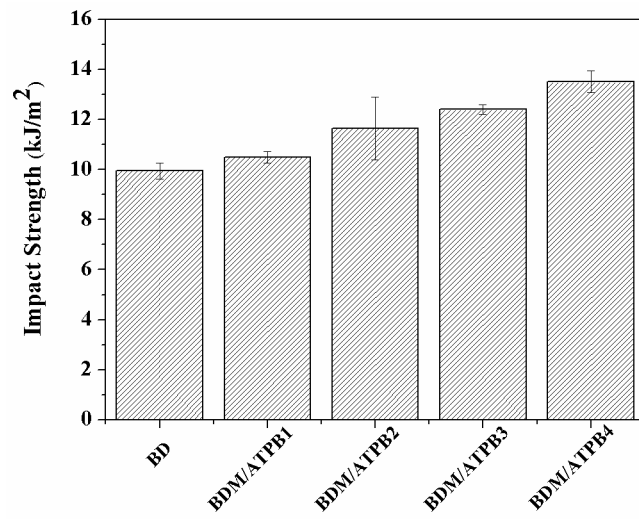


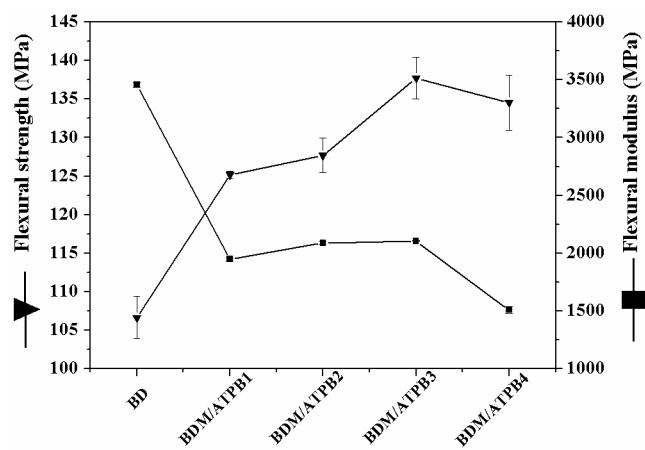












Supporting Information

**Green flame retarding bismaleimide resin with simultaneously good processing characteristics,
high toughness and outstanding thermal stability based on a multi-functional organic boron
compound**

Yanjing Zhu, Li Yuan, Guozheng Liang*, Aijuan Gu*

Jiangsu Key Laboratory of Advanced Functional Polymer Design and Application

Department of Materials Science and Engineering

College of Chemistry, Chemical Engineering and Materials Science

Soochow University, Suzhou, Jiangsu 215123, China

*Corresponding author

Tel: +86 512 65880967

Fax: +86 512 65880089

E-mail: lgzheng@suda.edu.cn (G. Liang), or ajgu@suda.edu.cn (A. Gu).

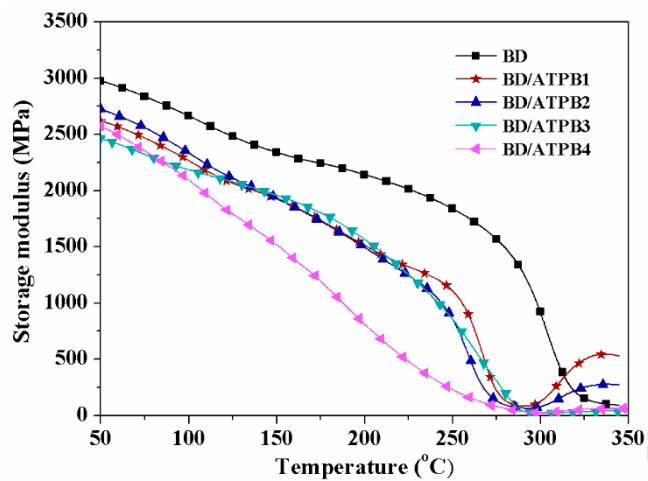


Figure SI-1. Overlay curves of storage modulus as a function of temperature for cured BD and BDM/ATPB resins.